Published in Appl. Phys. Lett. 97, 123110 (2010).

Electronic States of InAs/GaAs Quantum Dots by Scanning Tunneling Spectroscopy

S. Gaan, Guowei He, and R. M. Feenstra
Dept. Physics, Carnegie Mellon University, Pittsburgh, PA 15213

J. Walker and E. Towe
Dept. Electrical and Computer Engineering, Carnegie Mellon University, Pittsburgh, PA 15213

Abstract

InAs/GaAs quantum-dot heterostructures grown by molecular-beam epitaxy are studied using cross-sectional scanning tunneling microscopy and spectroscopy. Individual InAs quantum dots (QDs) are resolved in the images. Tunneling spectra acquired 3-4 nm from the QDs show a peak located in the upper part of the GaAs bandgap originating from the lowest electron confined state, together with a tail extending out from the valence band from hole confined states. A line-shape analysis is used to deduce the binding energies of the electron and hole QD states.

Semiconductor quantum dots (QDs) are highly interesting owing to nm-scale charge carrier confinement in all three spatial dimensions. This gives rise to quantized energy of the QDs[1] and associated applications such as lasers, photodetectors, or memory elements for quantum computers. Scanning tunneling microscopy (STM) has been used in many prior studies to probe the structural aspects of QDs, both in plan-view for viewing uncapped dots and in cross-section for viewing capped dots.[2,3,4,5,6,7,8] Scanning tunneling spectroscopy (STS) measurements during such studies are less common, and in some cases these works describe simply a reduced band gap associated with the dots.[2,3,8] A detailed interpretation of this band gap reduction is not clear *i.e.* particularly for relatively small dots in which discrete confined state features are expected to occur in the measured spectrum. In two exceptional works,[5,6] discrete electron and hole confined states have been observed by low-temperature STM/S. But even in these cases the energies of electron and hole QD states were not quantitatively determined, partly because of spectral distortion arising from tip-induced band bending in the semiconductor.

In this work we determine the size, shape, composition, and electronic properties of $In_xGa_{1-x}As$ QDs in GaAs using STM/S. The QDs are exposed on a (110) cleavage face of the wafer, revealing lens-shaped QDs with maximal diameter of 10.5 nm and height of 2.9 nm. Tunneling spectra are acquired at various distances from the QDs. At 3-4 nm from a QD the spectra reveal a distinct feature arising from the lowest electron confined state of the dot, along with conductance tail extending out from the valence band arising from hole confined states. The energies of the states are determined using a detailed 3D electrostatic simulation of the tip-vacuum-semiconductor geometry[9] together with computations of the tunnel current using a plane-wave method. We deduce a binding energy for the lowest electron (highest hole) state of 0.20 eV (0.19 eV), with these values found to be in agreement with optical spectroscopy measurements.

Our InAs/GaAs QD structures were grown using solid source MBE. On a heavily doped (1×10^{18} cm^{-3}) n-type (001) oriented GaAs substrate, 200 nm of GaAs buffer layer was grown followed by 5 periods of InAs QDs. The QD layers were separated by 50 nm of GaAs. The superlattice was then capped with about 200 nm of GaAs overlayer. All layers are undoped. Each layer of QDs consists of ≈2.7 ML of InAs deposited in a time of 10 s, with the sample at 490°C. STM measurements were performed at room temperature in an ultra high vacuum chamber with base pressure $<5\times10^{-11}$ Torr. Samples were cleaved *in-situ* to expose atomically flat (110) surfaces. Commercial Pt-Ir tips were cleaned *in-situ* by electron bombardment prior to use. Images were acquired with a constant current of 0.1 nA, and at sample-tip voltages specified below. Conductance spectra were measured and normalized in the same manner as previously described.[9]

Figures 1(a) and (b) show STM images of the the InAs/GaAs heterostructure. Individual QDs together with an interdiffused wetting layer are seen, and in Fig. 1(a) an atomic step formed due to *in-situ* cleaving process appears on the left-hand side of the image. The QDs appear bright in the images because, after cleavage, they relax outwards due to the strain arising from the 7% lattice mismatch between InAs and GaAs. An image of the QD from the lower part of Fig. 1(a) is shown after high-pass filtering in Figs. 1(c) and (d). The cross-sectional shape of the QDs is seen to be consistent with either a

truncated pyramid, a truncated cone, or a lens (section of a sphere),[4,7] with sidewalls having angle of ≈55° from the base. Following the methodology of Bruls *et al.*[4] we plot a distribution of heights and base lengths for images such as Fig. 1(c) from which we determine that the QD shape is consistent with either a truncated cone or a lens, and we use the latter for further analysis. The maximum base length along the $[1\bar{1}0]$ direction and height along the [001] direction were found to be 10.5±0.5 and 2.9±0.2 nm, respectively (the height *includes* the wetting layer). Analysis of both topographic profiles and local lattice parameter through the QDs reveals a distribution of In content, varying from 65% at the base of the QD to 95% at its center and back to 65% at its apex. This analysis will be described in detail elsewhere.

Spectra were acquired at various distances from the QDs; typical data are shown in Fig. 2. Let us first examine spectrum A, acquired sufficient far (6 nm) from the QD so that the result is representative of the bare GaAs(110) surface. A bandgap region is apparent in the spectrum, extending from about -0.5 to $+1.0$ V. Examining the spectra as the dot is approached, we observed in spectra C-E (and weakly in K) the appearance of the discrete state located ~0.2 eV below the GaAs conduction band (CB) edge. This peak is relatively sharp and well-defined, and we associate it with the lowest electron confined state of the QDs. However, at spatial locations closer to the dot, it is seen that this peak broadens substantially. Directly on the QD, spectrum G, we can no longer resolve the discrete state, but rather, the spectrum displays simply an apparent reduced-size bandgap of ~0.8 eV. We propose that this dramatic change in the spectra occurs due to the large currents passing through the dots, which causes significant occupation of the (normally empty) electron confined states. Occupation of the dot produces typically a 25 meV shift in the energy of the confined state,[10] so occupation by several electrons would be consistent with our observations. We note that charging of QDs has been observed in other experimental situations as well.[11]

To quantify the energy of the observed QD electron state we compare the experimental data with computed spectra, adjusting the band offsets (and hence the energy of confined states) to match theory and experiment. The computations are performed in a similar manner as for our prior determination of band offsets in InGaP/GaAs heterojunctions,[9] except that for the present problem of a QD we employ a plane wave expansion method for solving the Schrödinger equation. Free parameters in the computation include the tip-sample separation *s*, the tip radius-of-curvature *R*, and the sample-tip contact potential $\Delta\phi$ (*i.e.* their work-function difference). To match the computations to experiment, we also find it is necessary to introduce an extrinsic surface charge density associated with to the presence of atomic steps on the surface. One such step is seen ≈6 nm from the QDs of Fig. 1(a) and Fig. 2, and generally we observe 1 or 2 steps near each layer of QDs. The steps have midgap states that are spectrally resolved in Fig. 2(L), acting to pin the surface Fermi-level at an energy slightly above the valence band (VB) maximum. We model the steps with a constant state-density across the gap of density σ, and with charge neutrality level E_N. We obtain good fits for state-densities close to one dangling bond per unit cell length along the step (0.4 nm) per eV, 2.5 $\mathrm{nm^{-1}eV^{-1}}$, which seems quite reasonable.

A comparison of measurement and computed spectra is shown in Fig. 3, using spectra A and C from Fig. 2 but now plotted using the conductance at constant tip-sample separation. We fit both spectra simultaneously to the theory. At 6 nm from the QD [Fig. 3(a)] the states of the dot make almost no contribution to the spectrum, whereas the spectrum acquired 4 nm from the QD [Fig. 3(b)] clearly shows features from electron and hole confined states. These features can be fit using our parameters for the CB and VB band offsets, ΔE_V and ΔE_C (the offsets are taken to be proportional to the In content in the QD, with values quoted here corresponding to 100% In). The tail extending out from the VB for the QD spectrum is found to arise from a confined light-hole state, and the peak ~0.2 V below the CB edge comes from a confined electron state. However, using only the band offsets, we obtain a deep minimum in the computed conductance near +1.1 V, with theory being about 10× less than experiment. The reason for this discrepancy is that the *number* of electron and hole states is significantly underestimated in our effective-mass theory,[12] and utilizing only the band offsets we obtain just a single QD electron state. To achieve a better fit to the experiment we therefore introduce one additional parameter, a scale factor α by which we increase the QD size and thus introduce more states into the computed spectrum (in the fitting procedure, the band offsets are reduced as α is increased in order to maintain approximately constant energies for the lowest electron and highest hole states). As shown by the open circles in Fig. 3(b), we now achieve a good fit to the experiment, with a second QD electron state occurring just below the CB edge.

The deduced values of the band offsets are model dependent, so we instead consider the actual binding energies of the QD states. These are extracted by performing an identical computation but *without* the presence of the electrostatic potential from the probe tip or the surface steps. We find binding energies of 0.196±0.012 and 0.185±0.023 eV for the lowest electron and highest hole confined states, respectively (the latter is a heavy-hole state). It has been recently demonstrated by Urbieta *et al*. that the energy of such states vary only slightly between an embedded dot and a cleaved dot,[6] so we can meaningfully compare our observed energies with measured results for embedded dots. Low-temperature (77 K) photoluminescence spectra from our samples reveals a peak emission wavelength of 1.12 μm = 1.11 eV (very similar to that obtained in our prior work[13]). Excitonic effects are relatively small,[1] at least for the size of QDs considered here, so this energy represents the difference between lowest electron and highest hole confined state energies. With the bandgap of GaAs decreasing by 5.4% as the temperature is raised to room temperature,[14] we estimate this energy difference to be 1.05 eV at room temperature. From our STS results we obtain an energy difference between electron and hole states of 1.42 – (0.196±0.012) – (0.185±0.023) = 1.039±0.026 eV, in agreement with the optical result.

In summary, we find that tunneling spectra from cleaved InAs QDs are greatly perturbed by charging of the dots. However, with the use of low tunnel currents (accomplished in our case by placing the tip 3-4 nm from the QD) it is possible to observe discrete features arising from the QD confined states. For a lens-shaped dot with average In composition of 80% and having base diameter of 10.5 nm and height 2.9 nm,

we find binding energies of 0.20 and 0.19 eV for the deepest electron and hole states, respectively. These values are in good agreement with energy gap seen in optical spectroscopy. An advantage of STS compared to optical spectroscopy is that *individual* energies of VB and CB states are obtained (rather than energy differences), and furthermore the measurement can be done on specific QDs whose size, shape, and composition are also determined. The present work was performed at room temperature; the use of low temperatures (and small modulation voltages) can certainly improve the resolution of the spectra,[5,6] but the computational methodology described here is still necessary in order to achieve a quantitative determination of binding energies from the tunneling spectra.

This work was supported by the National Science Foundation, grant DMR-0856240. Computing resources were provided by the McWilliams Center for Cosmology at Carnegie Mellon University. Discussions with H. Eisele, R. Goldman, and B. Grandidier are gratefully acknowledged.

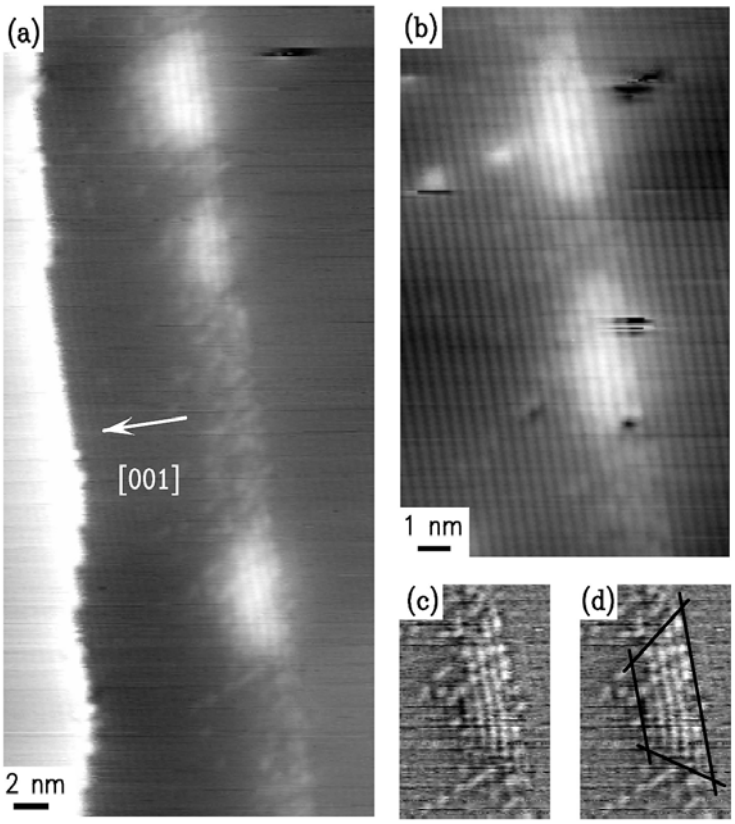

FIG 1. (a) and (b) STM images of InAs/GaAs QDs. The [001] growth direction is the same for both images, as indicated in (a). A step edge is seen in (a) that runs nearly parallel to the row of QDs. Both images were acquired with sample voltage of -2 V, and are displayed with gray scale ranges of 0.24 and 0.20 nm, respectively. (c) and (d) High-pass filtered view of the lower QD from (a), with an outline of the dot shown in (d).

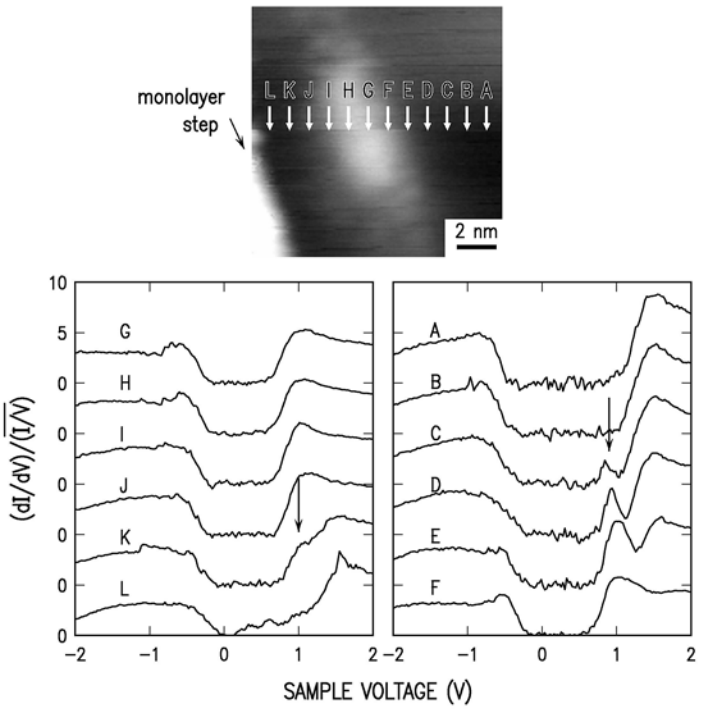

FIG 2. STM image (upper) and associated tunneling spectra (lower) of InAs QD. Spectra were acquired at the locations marked A-L in the image, with neighboring locations separated by 1.0 nm. A spectral peak associated with the dot is marked by the arrows, for spectra 3-4 nm from the dot.

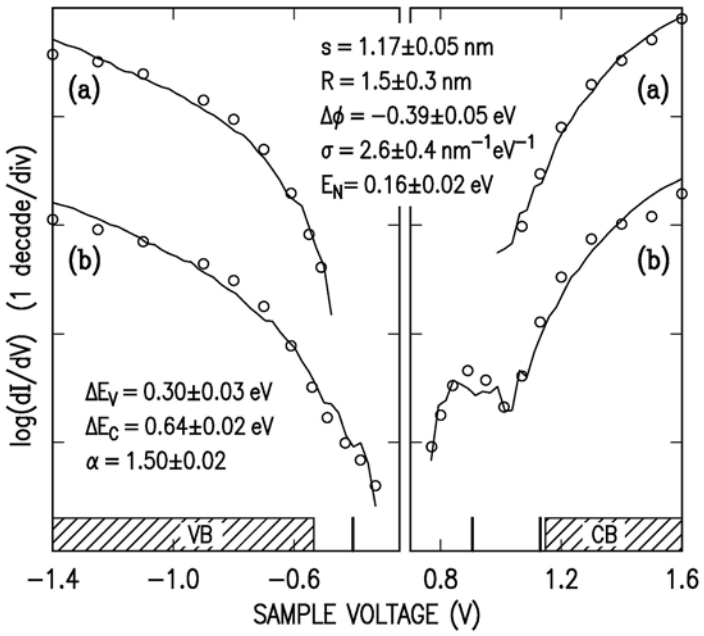

FIG 3. Conductance curves, acquired (a) 6 nm from the QD and (b) 4 nm from the QD. Experimental results are shown by lines and theoretical fits by circles. The curves (a) and (b) are shifted from each other for ease of viewing. Values for the fitting parameters are listed. The location of states from the theory is shown at the bottom of the figure, giving the voltages at which the tip Fermi-level is aligned with QD states (for the VB, only light-hole states are shown) and with the hatched regions showing unconfined VB and CB states in the near-surface region.

References:

[1] D. Bimberg, M. Grundmann, and N.N. Lendentsov, *Quantum Dot Heterostructures* (Wiley, New York, 1998).

[2] B. Legrand, B. Grandidier, J.P. Nys, D. Stiévenard, J.M. Gérard, and V. Thierry-Mieg, Appl. Phys. Lett. **73**, 96 (1998).

[3] T. Yamauchi, Y. Matsuba, L. Bolotov, M. Tabuchi, and A. Nakamura, Appl. Phys. Lett. **77**, 4368 (2000).

[4] D. M. Bruls, J. W. A. M. Vugs, P. M. Koenraad, H. W. M. Salemink, J. H. Wolter, M. Hopkinson, M. S. Skolnick, Fei Long, and S. P. A. Gill, Appl. Phys. Lett. **81**, 1708 (2002).

[5] T. Maltezopoulos, A. Bolz, C. Meyer, C. Heyn, W. Hansen, M. Morgenstern, R. Wiesendanger, Phys. Rev. Lett. **91**, 196804 (2003).

[6] A. Urbieta, B. Grandidier, J. P. Nys, D. Deremes, D. Stiévenard, A. Lemaître, G. Patriarche, and U. M. Niquet, Phys. Rev. B **77**, 155313 (2008).

[7] H. Eisele, A. Lenz, R. Heitz, R. Timm, M. Dähne, Y. Temko, T. Suzuki, and K. Jacobi, J. Appl. Phys. **104**, 124301 (2008).

[8] V. D. Dasika, R. S. Goldman, J. D. Song, W. J. Choi, N. K. Cho, and J. I. Lee, J. Appl. Phys. **106**, 014315 (2009).

[9] Y. Dong, R. M. Feenstra, M. P. Semtsiv, and W. T. Masselink, J. Appl. Phys. **103**, 073704 (2008). In the present work values of κ are taken from experiment, with a voltage-averaged value of $\kappa \approx 7.5$ nm^{-1}.

[10] O. Stier, M. Grundmann, and D. Bimberg, Phys. Rev. B **59**, 5688 (1999).

[11] K. H. Schmidt, G. Medeiros-Riberio, and P. M. Petroff, Phys. Rev. B **58**, 3597 (1998).

[12] L. W. Wang, A. J. Williamson, A. Zunger, H. Jiang, and J. Singh, Appl. Phys. Lett. **76**, 339 (2000).

[13] D. Pal and E. Towe, Appl. Phys. Lett. **88**, 153109 (2006).

[14] *Semiconductors: group IV elements and III-V compounds*, ed. O. Madelung, (Springer-Verlag, Berlin, 1991).